$$\tilde{g}_i(\beta) = \frac{1 + \epsilon_i \coth(\beta t_i)}{\beta\{\epsilon_i[\epsilon_i + \coth(\beta t_i)] + \epsilon_s \coth(\beta d)[1 + \epsilon_i \coth(\beta t_i)]\}}$$

and $i = 1$ or 2, corresponding to Fig. 1(a) or (b), respectively.

When a perturbation technique is used for the microstrip line filled with the materials that have small losses ($\sigma \ll \omega\epsilon$), the following expression for the line conductance G_i can be derived from (6):

$$\frac{G_i}{C_i^2} = \frac{1}{2\pi\epsilon_0 q^2}\int_{-\infty}^{\infty} \frac{\{\sigma_i[2\epsilon_i + (1+\epsilon_i^2)\coth(\beta t_i)] + \sigma_s \coth(\beta d)[1 + \coth(\beta t_i)]^2\}}{\beta\{\epsilon_i[\epsilon_i + \coth(\beta t_i)] + \epsilon_s \coth(\beta d)[1 + \epsilon_i \coth(\beta t_i)]\}^2} \cdot \tilde{\rho}^2(\beta)\, d\beta, \qquad i = 1 \text{ or } 2 \tag{7}$$

where σ_s and σ_i are the conductivities of the substrate and the loading material, respectively.

ACKNOWLEDGMENT

The author wished to thank Prof. J. D. Dyson and Prof. R. Mittra for fruitful discussions, and M. Sato and J. J. Sweeney for experimental assistance.

REFERENCES

[1] J. S. Yu, L. Peter, Jr., and D. A. Castello, "A refractive index chart for a scattering sphere," *IEEE Trans. Antennas Propagat.*, vol. AP-18, pp. 75–83, Jan. 1970.
[2] D. J. Burr, "Measurement of the complex dielectric constant from resonance in the radar cross section of a dielectric sphere," M.S. thesis, Dep. Elec. Eng., Univ. Ill., Urbana, 1971.
[3] H. E. Stinehelfer, Sr., "Ridge waveguide resonant cavity for measuring dielectric constants," *Patent Gazette*, 3,384,814, May 21, 1968.
[4] M. Olyphant, Jr., and J. H. Ball, "Strip-line method for dielectric measurements at microwave frequency," *IEEE Trans. Elec. Insul.*, vol. EI-5, pp. 26–32, Mar. 1970.
[5] L. S. Napoli and J. J. Hughes, "A simple technique for the accurate determination of the microwave dielectric constant for microwave integrated circuit substrates," *IEEE Trans. Microwave Theory Tech.* (Corresp.), vol. MTT-19, pp. 664–665, July 1971.
[6] J. Q. Howell, "A quick accurate method to measure the dielectric constant of microwave integrated-circuit substrates," *IEEE Trans. Microwave Theory Tech.* (Short Paper), vol. MTT-21, pp. 142–143, Mar. 1973.
[7] P. H. Ladbrooke, M. H. N. Potok, and E. H. England, "Coupling errors in cavity-resonance measurements on MIC dielectrics," *IEEE Trans. Microwave Theory Tech.* (Short Paper), vol. MTT-21, pp. 560–562, Aug. 1973.
[8] R. Mittra and T. Itoh, "A new technique for the analysis of the dispersion characteristics of microstrip lines," *IEEE Trans. Microwave Theory Tech.*, vol. MTT-19, pp. 47–56, Jan. 1971.
[9] S. Ramo and J. R. Whinnery, *Fields and Waves in Modern Radio.* New York: Wiley, 1953.
[10] T. Itoh, R. Mittra, and R. D. Ward, "A method for computing edge capacitance of finite and semifinite microstrip lines," *IEEE Trans. Microwave Theory Tech.* (Short Paper), vol. MTT-20, pp. 847–849, Dec. 1972.
[11] H. A. Wheeler, "Transmission-line properties of parallel strips separated by a dielectric sheet," *IEEE Trans. Microwave Theory Tech.*, vol. MTT-13, pp. 172–185, Mar. 1965.
[12] H. E. Stinehelfer, Sr., "An accurate calculation of uniform microstrip transmission lines," *IEEE Trans. Microwave Theory Tech.* (*Special Issue on Microwave Integrated Circuits*), vol. MTT-16, pp. 439–444, July 1968.
[13] E. Yamashita and R. Mittra, "Variational method for the analysis of microstrip lines," *IEEE Trans. Microwave Theory Tech.*, vol. MTT-16, pp. 251–256, Apr. 1968.
[14] E. Yamashita, "Variational method for the analysis of microstrip-like transmission lines," *IEEE Trans. Microwave Theory Tech.*, vol. MTT-16, pp. 529–535, Aug. 1968.

Circular Bends in Dielectric Frame Beam Waveguides

P. F. CHECCACCI, R. FALCIAI, AND A. M. SCHEGGI

***Abstract*—An investigation is described on circular bends in beam waveguides constituted by dielectric frames [5]. A uniform bending of the guide axis is obtained by tilting each frame by a small angle; however, due to the phase correction performed by the dielectric frame, the losses introduced by the bending can be made lower than those of an analogously bent iris waveguide. A numerical analysis is performed on the basis of the analogy between beam waveguides and open resonators which permits the assessment, in a number of cases, of the maximum permissible amount of tilting and the corresponding optimum frame dimensions in view of acceptable losses. The losses due to mode conversion are also evaluated when considering the connection between a straight and a curved section of the waveguide.**

Manuscript received September 12, 1973; revised January 3, 1974.
The authors are with Consiglio Nazionale Delle Ricerche, Istituto di Ricerca sulle Onde Eletromagnetiche, Florence, Italy.

It is well known that beam waveguides cannot be made to follow a curved path like tubular waveguides, but bends can be obtained by the use of prisms or mirrors. However, curvatures with large radii (like those encountered to follow the ground contour or to avoid obstacles along the path) can be achieved by lateral displacements of the elements in a lens waveguide or by a sequence of small angle changes at each aperture of an iris waveguide [1]–[4].

The present short paper is concerned with an investigation of circular bends in dielectric frame beam waveguides [5], [6], along with some considerations on the transition between straight and curved sections of the guide.

The investigation has been carried out on the basis of the analogy between open resonators and beam waveguides. In this respect it is expedient to recall that the dielectric frame beam waveguide is equivalent to the step rimmed Fabry–Perot resonator [6], [7]. The rims control the field at the edges of the mirrors giving rise to a periodical enhancement or decrease of the losses as the rim thickness varies. Such control can also be made at each edge almost independently and without altering appreciably the overall field shape.

A beam waveguide of constant radius of curvature is equivalent to a tilted rimmed mirror resonator. The diffraction losses for the fundamental mode of a Fabry–Perot resonator with tilted mirrors have been evaluated for different amounts of tilting and by varying the Fresnel number. Such losses (Fig. 1) have been compared with those evaluated for the same resonators in the presence of rims. The rim dimensions (width and thickness) here are those corresponding to minimum loss and, in fact, the losses of the rimmed resonator are much lower than those in the absence of rim. This decrease is due to the rims placed at the largest distance edges of the mirrors which limit the field spill-over caused by the tilting. Equal curves are obtained by placing the rims also at the nearest distance edges, their effect being negligible due to the extremely low value of the field at that side. Consequently, this rim can be suppressed; however, when considering the corresponding beam waveguides (Fig. 2), this rim is maintained for constructive reasons and the curved section waveguide results constituted by a number of cells with frames tilted one with respect to the other by the same angle. The guidance in such curved sections is achieved through the combined effects of frame tilting and phase-front correction performed by the frame itself at the external side of the curve.

The diffraction losses per cell are those of the equivalent resonator (Fig. 1). However, other losses are present, and precisely, losses due to mode conversion at the transition between straight and curved sections and vice versa, as well as reflection losses due to impedance mismatching at the same transitions. These last ones will be neglected in our treatment. The mode conversion losses of interest in this case are those relative to the zero mode which at the transitions is partially converted into higher order ones. The energy lost in this conversion was evaluated by considering the ratio between the energy of the zero mode for the input cell and the energy of the resultant zero mode of the output cell.

Fig. 3 shows the mode conversion losses in the case $N = 2.5$ plotted versus ϵ (amount of tilting of the output cell) for different values of ϵ_0 (amount of tilting of the input cell). The value $\epsilon_0 = 0$ corresponds to the particular case of a transition between a straight and a tilted cell. Values of the radii of curvature corresponding to the considered values of ϵ_0 and ϵ are also indicated which are valid in

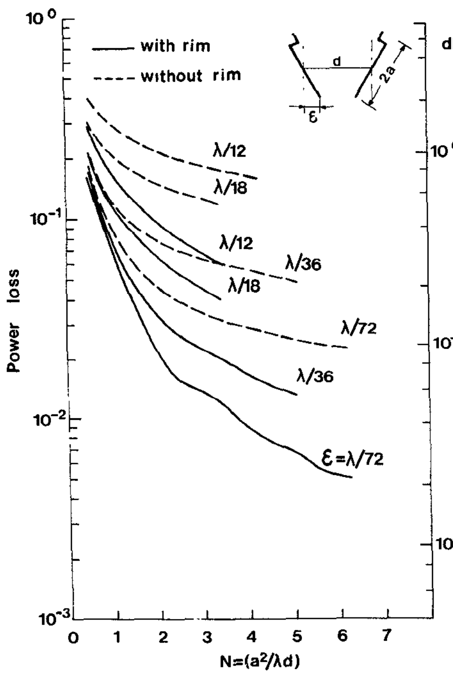

Fig. 1. Diffraction power losses of a tilted mirror Fabry–Perot resonator for different amounts of tilting, with and without rims, at the largest distance edges of the mirrors, versus Fresnel number.

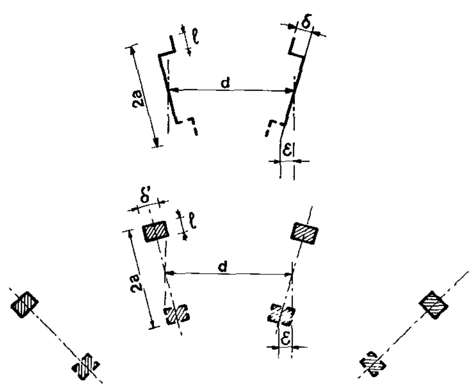

Fig. 2. The tilted mirrors resonator with a rim at the largest distance edges and the equivalent beam waveguide.

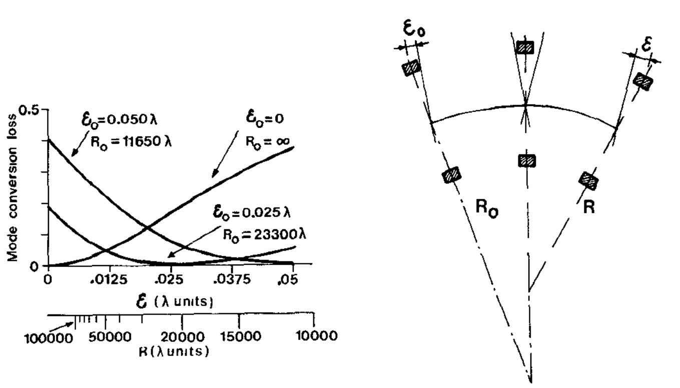

Fig. 3. Mode conversion losses at the transition between two differently tilted cells plotted versus amount of tilting ϵ. The lower scale is valid for the case $2a = 28.6\lambda$; $d = 81.3\lambda$. $N = 2.5$.

the case $N = 2.5$ with $2a = 28.6\lambda$, $d = 81.3\lambda$. These curves give also the mode conversion losses for the inverse transition (for instance from a tilted to a parallel cell). In the considered range of tilting, the mode conversion losses turn out to be much higher than the diffraction losses per cell, so that they are important only for short curved sections.

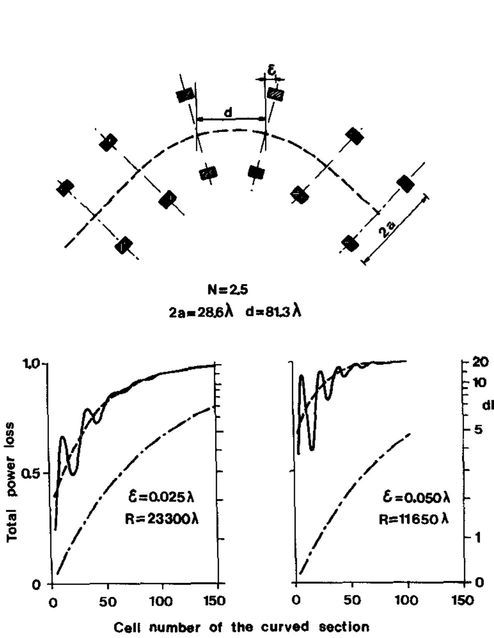

Fig. 4. Two examples of curved sections connecting two straight waveguides: diffraction plus mode conversion losses plotted versus number of cells (continuous and dotted lines) compared with the losses of straight sections of equal lengths (dotted–dashed lines).

Finally, two typical examples of curved sections were considered. Again, with Fresnel number $N = 2.5$, the cases were examined of curved sections connecting two straight waveguides with cells tilted by $\epsilon = 0.025\lambda$ and $\epsilon = 0.05\lambda$, respectively.

Fig. 4 shows the total power losses for the zero mode (diffraction plus conversion losses) evaluated directly when the number of cells varies. The dotted curves correspond to the same losses estimated on the basis of the values given by the curves of the diffraction and mode conversion losses. For a high number of cells the two curves coincide because all the higher modes are vanishing due to the section length; consequently, the input and exit transitions result independently. For a lower number of cells, due to the interference among the zero mode and the other modes, the conversion losses at the second transition depend on the particular considered cell and, hence, the loss curve oscillates. The dotted–dashed line corresponds to the losses of a straight waveguide section constituted by the same number of cells as the curved section. One can observe that the loss increase due to curvature is still acceptable, especially taking into account the small values of R in the considered examples. For instance, an angle of 20° can be made with a section of 100 cells with $R = 23\,300\lambda$ or with a section of 50 cells with $R = 11\,650\lambda$. The resultant loss increases are 8.5 and 12.8 dB, respectively.

In conclusion, the performed analysis has shown that circular bends can be obtained in dielectric frame beam waveguides with reasonably small radii of curvature, by simply tilting one frame with respect to the other by a small angle. Due to the phase front correction performed by the frame at the external side of the curve, the diffraction losses are lower than those of an equally curved iris waveguide section. The mode conversion losses evaluated on the basis of the ratio between the energy of the zero-order modes at the two sides of the transition between two differently tilted cells are relevant in comparison with diffraction losses per cell. However, the higher the number of cells constituting the curved section, the less important become the mode conversion losses.

REFERENCES

[1] D. Marcuse, "Propagation of light rays through a lens-waveguide with curved axis," *Bell Syst. Tech. J.*, vol. 44, p. 2065, 1965.
[2] G. Goubau, *Beam Waveguides—Advances in Microwave*. New York: Academic, 1968, pp. 110–123.
[3] J. W. Mink, "Experimental investigation with an iris beam waveguide," *IEEE Trans. Microwave Theory Tech.* (Corresp.), vol. MTT-17, pp. 48–49, Jan. 1969.
[4] ——, "Assessment of optical iris-beam waveguides," *Electron. Lett.*, vol. 7, p. 527, 1971.
[5] P. F. Checcacci and A. M. Scheggi, "Dielectric frame beam waveguide," *Proc. IEEE* (Lett.), vol. 59, pp. 1024–1025, June 1971.
[6] P. F. Checcacci, R. Falciai, and A. M. Scheggi, "Phase step beam

waveguide," *IEEE Trans. Microwave Theory Tech.*, vol. MTT-20, pp. 608–613, Sept. 1972.
[7] P. F. Checcacci, A. Consortini, and A. M. Scheggi, "Effect of mirror rims on modes and losses of a planar Fabry-Perot resonator," *Appl. Opt.*, vol. 10, p. 1363, 1971.
[8] P. F. Checcacci and A. M. Scheggi, "Open resonators with rimmed mirrors," in *Proc. European Microwave Conf.*, Sept. 1969.
——, "Open resonators with rimmed mirrors," in *1969 Inst. Elec. Eng. Conf. Publ. No. 58*, p. 314, 1969.

Q Degradation in Varactor-Tuned Oscillators

S. F. PAIK, MEMBER, IEEE

***Abstract*—A general analysis of varactor-tuned negative-resistance oscillators is presented to show the varactor loading effect on the oscillator Q. The external Q of the varactor loaded circuit normalized with respect to the unperturbed external Q is plotted as a function of the tuning range for several values of the varactor Q and the capacitance ratio.**

In varactor-tuned oscillators, the primary factor limiting the tuning range is the resistive loading effect of the varactor diode. As the diode is coupled strongly into the oscillator circuit, the tuning range increases at the expense of the oscillator Q. The tuning range attainable with a given diode, therefore, is determined by the allowable degradation of the oscillator Q and the accompanying power dissipation. Cawsey [1] has presented an analytical evaluation of this effect, but his results did not include an explicit relation between the oscillator Q and the tuning range. Inasmuch as several critical parameters of oscillators, such as the FM noise and the temperature stability, are directly related to the external Q of the oscillator, it is desirable to have a quantitative measure of the tradeoff between the oscillator Q and the tuning range. In this note, we present an analysis of varactor-tuned negative-resistance oscillators and derive a general expression for the external Q as a function of the commonly quoted varactor parameters and the tuning range.

Fig. 1 shows circuit models of a varactor-tuned negative-resistance oscillator (e.g., IMPATT or Gunn diode oscillators). In practice, both the varactor and the load may be coupled to the negative-resistance element through a transformer, and the circuit parameters indicated in Fig. 1 refer to transformed quantities. Following the common practice, the varactor diode is represented by a series RC circuit, in Fig. 1(a), and all parasitic elements are assumed to be included in the main resonator. This equivalent circuit is valid at frequencies near resonance if the varactor impedance (including the package parasitics) is a smooth function of frequency and bias voltage devoid of loops in the impedance plot.

The varactor capacitance C_V is a function of the bias voltage, decreasing monotonically from C_{V0} at zero bias to C_{VB} at breakdown. The series resistance R_S is assumed to be constant at all bias levels. Varactors are usually characterized by two invariant parameters defined in terms of C_V and R_S: r, the capacitance ratio, and its quality factor Q_V:

$$r = \frac{C_{V0}}{C_{VB}} > 1 \tag{1}$$

$$Q_V = \frac{1}{(\omega R_S C_{V0})}. \tag{2}$$

Since the oscillator circuit in Fig. 1 is represented by a shunt resonant circuit, it is convenient to convert the varactor into its shunt equivalent form as shown in Fig. 1(b). The shunt elements are

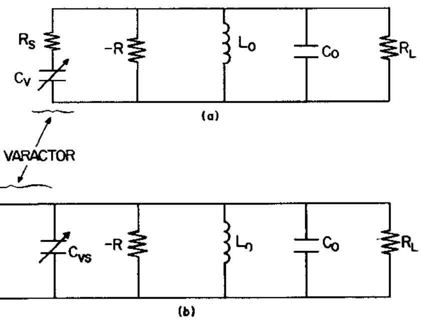

Fig. 1. (a) Equivalent circuit of a varactor-tuned negative-resistance oscillator with the varactor represented by a series RC circuit. (b) With the varactor represented by a parallel RC circuit.

$$G_S = \left(\frac{1}{R_S}\right)\left[1 + Q_V^2\left(\frac{C_{V0}}{C_V}\right)^2\right]^{-1} \simeq \left[R_S Q_V^2 \left(\frac{C_{V0}}{C_V}\right)^2\right]^{-1} \tag{3}$$

$$C_{VS} = C_V[1 + (C_V/C_{V0})^2/Q_V^2]^{-1} \simeq C_V. \tag{4}$$

The approximation is valid if $Q_V^2 \gg 1$.

In the absence of the varactor, the resonant frequency and the external Q of the oscillator are

$$\omega_0 = (L_0 C_0)^{-(1/2)} \tag{5}$$

$$Q_{\text{ext}} = \omega C_0 R \tag{6}$$

where

$$R = |-R| = R_L.$$

When the varactor is introduced, the frequency of the oscillation can be tuned from

$$\omega_1 = [L_0(C_0 + C_{V0})]^{-(1/2)}$$

to

$$\omega_2 = [L_0(C_0 + C_{VB})]^{-(1/2)}.$$

Assuming the difference between C_{V0} and C_{VB} is a small fraction of the total capacitance $(C_0 + C_{V0})$, the fractional tuning range referenced to ω_1 may be expressed as a function of the capacitance ratio as follows:

$$\Delta f/f_1 \simeq (1/2)[(C_{V0} - C_{VB})/(C_0 + C_{V0})] = \frac{1}{2}\frac{(1 - 1/r)}{(1 + C_0/C_{V0})}. \tag{7}$$

The external Q of the varactor-tuned oscillator reaches its lowest value at zero bias, since the varactor at zero bias introduces the greatest perturbation and its own Q is at its lowest. The external Q of the oscillator at zero bias is

$$Q'_{\text{ext}} = \omega(C_0 + C_{V0})\left[\frac{R R_S Q_V^2}{R + R_S Q_V^2}\right] = \frac{Q_{\text{ext}} Q_V^2}{(R/R_S) + Q_V^2} + \frac{Q_V}{1 + (R_S/R) Q_V^2}. \tag{8}$$

This expression may be normalized with respect to the unperturbed external Q in terms of the capacitance ratio, the tuning range, and the normalized varactor Q using (2), (6), and (7):

$$\frac{Q'_{\text{ext}}}{Q_{\text{ext}}} = [1 + 2xr(q - 1)/(r - 1)]^{-1} \tag{9}$$

where

$$x = \Delta f/f_1$$

and

$$q = Q_{\text{ext}}/Q_V.$$

Manuscript received October 15, 1973; revised January 7, 1974.
The author is with the Special Microwave Devices Operation, Raytheon Company, Waltham, Mass. 02154.